

Münster-Müller Sascha (Orcid ID: 0000-0003-3949-2818)

**Chemical profiling of the synthetic cannabinoid MDMB-CHMICA: identification, assessment and stability study of synthesis-related impurities in seized and synthesized samples**

**\*Sascha Münster-Müller<sup>1,2</sup>, Steven Hansen<sup>3</sup>, Till Opatz<sup>3</sup>, Ralf Zimmermann<sup>2,4</sup>, Michael Pütz<sup>1</sup>**

<sup>1</sup>Federal Criminal Police Office, Forensic Science Institute, Äppelallee 45, 65203 Wiesbaden, Germany

<sup>2</sup>Joint Mass Spectrometry Centre, Institute of Chemistry, Chair of Analytical Chemistry, University of Rostock, 18057 Rostock, Germany

<sup>3</sup>Johannes Gutenberg University Mainz, Institute of Organic Chemistry, Duesbergweg 10-14, 55128 Mainz, Germany

<sup>4</sup>Joint Mass Spectrometry Centre, Cooperation Group “Comprehensive Molecular Analytics”, Helmholtz Zentrum Muenchen, 85764 Neuherberg, Germany

\*Sascha Münster-Müller, Bundeskriminalamt (Federal Criminal Police Office), Forensic Science Institute, Äppelallee 45, 65203 Wiesbaden, Germany. Email: Sascha.muenstermueller@uni-rostock.de

**Keywords:** new psychoactive substances (NPS); MDMB-CHMICA; impurity profiling; LC-MS; controlled synthesis

This article has been accepted for publication and undergone full peer review but has not been through the copyediting, typesetting, pagination and proofreading process which may lead to differences between this version and the Version of Record. Please cite this article as doi: 10.1002/dta.2652

## Abstract

In this work, the most discriminating synthesis-related impurities found in samples from seizures and controlled synthesis of the synthetic cannabinoid MDMB-CHMICA (methyl (*S*)-2-(1-(cyclohexylmethyl)-1*H*-indole-3-carboxamido)-3,3-dimethylbutanoate) were characterized. Based on sixty-one available powder samples of MDMB-CHMICA, fifteen key-impurities were assessed, isolated in larger quantities via flash-chromatography and structurally elucidated and characterized via HR-MS and NMR. Apart from verifying the relation of the impurities to the major component, the interpretation of their chemical structures with distinct structural elements provided first insights into the manufacturing process and the precursor compounds used. Following LC-MS analysis of the fifteen key-impurities, the sixty-one seized samples of MDMB-CHMICA were evaluated and classified via multivariate data analysis based on the corresponding relative peak areas. In a second part of this work stability tests and multiple controlled syntheses of MDMB-CHMICA were carried out to better understand variations in impurity signatures and to assess the significance of variations in the impurity patterns of seized samples. The last coupling step of the amino acid with 1-(cyclohexylmethyl)-1*H*-indole-3-carboxylic acid was performed using the coupling agents oxalyl chloride, thionyl chloride and HATU. Furthermore, the impact of reaction time and temperature on the impurity profile were investigated. Overall, eight new impurities were found in the controlled syntheses and two degradation products of MDMB-CHMICA were found in the course of the stability tests. Replicates of a synthesis conducted on the same day showed similar impurity signatures, on different days discriminable signatures. The use of different coupling reagents or conditions gave clearly distinguishable impurity signatures.

Accepted Article

## 1. Introduction

Seized samples of illicit drugs produced under clandestine lab conditions generally are complex mixtures of the main active ingredient and a variety of by-products, e.g. natural products from leaf extractions in the case of cocaine<sup>1-3</sup> or synthesis impurities of synthetic drugs like amphetamine<sup>4-7</sup>. It could be expected that samples originating from the same general process exhibit the same by-product profile. However, their overall presence and concentration may show large variations due to changes in the nature of the starting material, processing pathway, manufacturing parameters as well as distribution and storage conditions. The chromatographic separation and quantitative analysis of these by-products (impurity-profiling) is an often used method by forensic scientists contributing to several investigative purposes: to establish links between two or more seized samples; to classify material from different seizures into larger groups revealing potential distribution networks; to identify the geographical origin of a sample; to monitor the manufacturing procedures of clandestine laboratories<sup>8</sup>.

In the first step of common impurity-profiling workflows, the seized material is dissolved and impurities are separated from the main component by acid-base liquid-liquid extraction, followed by analysis of the enriched impurity extract via liquid or gas chromatography coupled to mass spectrometry (LC-MS or GC-MS)<sup>9-12</sup>. The integrated peak signals of a list of pre-defined key-impurities are then matched via chemometric models to databases of previously seized samples<sup>2,3,13,14</sup>. The decision whether two samples are somehow linked (e.g. come from the same synthesis, the same laboratory or the same synthesis route) or are not related to each other, requires a thoroughly assessed scientific basis, especially with respect to the legal defensibility of the profiling results. It is essential for the development of a valid and statistically robust profiling method to provide experimental studies demonstrating the relevance and eligibility of chosen key-impurities, their relation to the main component, at which point differences between sample profiles are significant and which magnitudes of influence can be responsible for these differences. Various publications are available detailing structural elucidation of impurities by MS-fragmentation experiments, high resolution MS (HR-MS) or nuclear magnetic resonance spectroscopy (NMR)<sup>5,15-18</sup>; controlled syntheses to assess route specific impurities and the overall reproducibility of the chemical profile<sup>6,17,19-21</sup>; stability tests to identify impacts on the profile of a drug sample as a result of different storing conditions, e.g. exposure to heat, sunlight or moisture, which could lead to a decomposition of the main component or related impurities<sup>22</sup>.

Several international impurity-profiling programmes for classical drugs are already validated<sup>13,23,24</sup> or in constant development to cope with changes in illicit drug manufacturing and distribution. For synthetic cannabinoids, stimulants (derived from phenethylamine) and opioids, all part of the new psychoactive substances (NPS) phenomenon, only few chemical profiling approaches are published.<sup>25-27</sup> Nevertheless, the number of newly detected NPS was rising every year up to 2018, with 899 individual substances being reported to the Early Warning Advisory (EWA) of the United Nations Office on Drugs and Crime (UNODC)<sup>28</sup>. This phenomenon grew to a major concern of the legislation and prosecution agencies all over the world. In Germany, the most popular NPS group comprises the synthetic cannabinoids, either sold as research chemicals (RC) in pure form as powders and more prevalent, applied onto a herbal matrix, called herbal blends or “Spice-products”<sup>29,30</sup>. Little is known about the production and distribution of these substances and the designer drug products made of them,

which is why a new profiling concept for this sub-class was developed in a previous paper to link seizures and to gain more insight in the manufacturing process like batch and synthesis pathway discrimination. Due to several differences between synthetic cannabinoids and classical drugs, like their much higher chemical purity and the non-applicability of acid-base liquid-liquid extraction for the isolation of active constituents, it was necessary to adapt the established profiling routines to a new workflow consisting of flash-chromatography, LC-MS and multivariate data evaluation<sup>31</sup>. A continuous database-supported monitoring and evaluation would not be reasonable for synthetic cannabinoids, as individual active substances typically do not stay on the market for more than one to two years<sup>32</sup>. For the same reason, the establishment of a broad scientific basis for the chemical profiling of every newly emerging synthetic cannabinoid would not be worth the effort. However, an in-depth analysis with focus on one highly prevalent cannabinoid could provide comprehensive insights into its clandestine synthesis and, thus, contribute to better understand the variations in the impurity composition of seized material and their significance for NPS-targeted forensic profiling applications in general. The methodological approach presented here will serve as model for the interpretation of impurities found by forensic institutes when analyzing seized synthetic cannabinoids with indole, indazole and carbazole core structures, as similar synthesis procedures with related reaction by-products are expected for newly arising specimens of these three sub-classes. In the presented work, the most discriminating key-impurities found in seized and bought (internet-test purchases) samples of the synthetic cannabinoid methyl (2S)-2-[[1-(cyclohexylmethyl)indole-3-carbonyl]amino]-3,3-dimethylbutanoate (**1**) (MDMB-CHMICA, Figure 1) were identified and structurally elucidated, MDMB-CHMICA being the most prevalent cannabinoid in 2016 in Germany<sup>30,33</sup> (and thus continued the previously published work on this compound<sup>31</sup>). Due to the high purity of the available samples of **1** (> 98%), it was necessary to isolate the synthesis impurities from the main component via flash-chromatography (F-LC). Tentative identification via fragmentation experiments and corresponding sum formula generation via high resolution mass spectrometry (HR-MS) was carried out and, if applicable, the most abundant impurities were isolated in larger quantities for structural elucidation via nuclear magnetic resonance spectroscopy (NMR)(Figure 1).

After the assessment of suitable target components in the first part of this work, controlled syntheses of **1** were carried out to better understand variations in impurity signatures and to assess the significance of variations in the impurity patterns of seized samples. The focus was put on what is presumably the last reaction step for most of the “modern” synthetic cannabinoids, the coupling of the amino acid moiety to the aminoalkylindole core, from a single batch of the precursor material 1-(cyclohexylmethyl)-1*H*-indole-3-carboxylic acid. Only hypothetical considerations are possible on how the clandestine manufacturers conduct their synthesis. Most probably, previously published procedures are tested, evaluated and modified to enable up-scaling from laboratory to pilot-plant scale and to improve the economic aspects of the synthesis. The scientific groundwork for the majority of the modern substances was laid by research groups beginning in the late 1980s, who developed new substances, that act on the human endocannabinoid system, for the pharmaceutical industry<sup>34-37</sup>. Most of the synthetic cannabinoids found on the market were directly described in these patents or papers, or at least were inspired by them with respect to the general synthesis procedures (e.g. exchange of

indazole core with indole for **1** or carbazole core for MDMB-CHMCZCA<sup>38</sup>), except for a few rare cases like 5F-PB-22<sup>39</sup>. Since no information on the actual synthesis routes employed by the manufacturers is available, the initial synthesis conditions were based on the patented version for the indazole analogue of **1** from Buchler et al.<sup>34</sup> and the parameters were adjusted, e.g. other coupling reagents, according to identified impurities found in the original seized samples. Three different synthesis variations were performed, using the coupling reagents [dimethylamino(triazolo[4,5-b]pyridine-3-yloxy)methylidene]-dimethylazanium hexafluorophosphate (HATU) as stated in the patent by Buchler et al. and additionally the chlorinating agents oxalyl chloride and thionyl chloride according to a highly abundant impurity (chlorinated derivative of MDMB-CHMICA), frequently observed in seized samples of MDMB-CHMICA. In two other synthesis procedures, the reaction time and temperature was varied for the coupling with oxalyl chloride. Only one factor was varied at a time, disregarding interaction between single parameters. However, compared to the manufacturers providing bulk material for the European market, the syntheses in this study were performed on a small scale. It was not intended to exactly reproduce the synthesis of the original manufacturer but to work as closely as possible to their assumed synthesis of choice.

## 2. Methods

### 2.1 Impurity Profiling

The complete impurity profiling workflow including sample preparation via flash-chromatography, UHPLC-MS and the subsequent data processing and multivariate data analysis was already reported in a previous paper<sup>31</sup> and will be stated in brief.

#### 2.1.1 Chemicals and samples

Deionized water was tapped by a Milli-Q Synthesis A10 device (Millipore, Schwalbach, Germany), hypergrade acetonitrile (MeCN) for LC-MS was purchased from Merck (Darmstadt, Germany), formic acid (~98%), ammonium formate (> 99 %), *n*-hexane (> 99.99 %) and ethyl acetate (≥ 99.0 %) from Fluka (Buchs, Switzerland).

Overall, sixty-one samples of pure **1** were available from a 40 kg seizure of Luxembourg customs in December 2014 (labeled as Lux), customs seizures in Finland (labeled as FL) and from test purchases in internet shops by the University Medical Center Freiburg (labeled as FR).

#### 2.1.2 Instruments

Separation of synthesis related impurities from the main component was achieved by normal phase preparative flash-chromatography with a Sepacore system X50 from Büchi Labortechnik (Flawil, Switzerland) consisting of two pump modules (max. 50 bar pressure), a UV-VIS spectrometer (set to 285 nm), an automated fraction collector and a control unit. Prepacked 4 g silica gel HP column from Büchi (particle size 15-40 µm) were used and run with mixtures of *n*-hexane and ethyl acetate as the mobile phase.

UHPLC measurements were conducted on a ternary system UltiMate 3000 by Dionex (Thermo Scientific, Waltham, MA, USA), consisting of a pump module, an autosampler and a column compartment. Separation was achieved on a Kinetex C18 (2.6 µm, 100 Å, 100 x 2 mm inner diameter) column from Phenomenex (Aschaffenburg, Germany) at 40 °C. Each analysis was

carried out with a binary mobile phase consisting of eluent A (98.9 % water, 1 % acetonitrile, 0.1 % formic acid, 2 mM ammonium formate) and eluent B (1 % water, 98.9 % acetonitrile, 0.1 % formic acid, 2 mM ammonium formate). For mass spectrometry, a Bruker amaZon Speed ion trap MS (Billerica, MA, USA) was operated in ultra-scan mode from 70-600 m/z with 32500 m/z/s. The dry gas flow rate was set to 10 L/min at a temperature of 320 °C

For high resolution measurements a LTQ Orbitrap hybrid MS with a “Max Ion Source” ESI or APCI ionization source, a LTQ XL ion trap and an Orbitrap (Thermo Scientific, Waltham, MA, USA) were used. Separation was done by an Accela-HPLC-Device with autosampler, HPLC-pump and photodiode array detector (Thermo Scientific, Waltham, MA, USA). For separation a gradient was applied of Eluent A (94.9:5:0.1 water : acetonitrile : formic acid) and Eluent B (94.9:5:0.1 acetonitrile : water : formic acid). The ESI operated in positive mode with 3.75 kV and the mass range of the mass spectrometer was set to 130-2000 m/z with a data dependent scan threshold for MS<sup>2</sup> of 10<sup>6</sup> counts. The instrument was calibrated by measuring crystal violet and comparing the measured m/z values to the theoretical. If deviations > 5 ppm occur, the instrument was recalibrated.

NMR spectra were recorded on a Bruker Avance-II 400 (400 MHz for <sup>1</sup>H NMR and 100.6 MHz for <sup>13</sup>C NMR, including 2D NMR) or on a Bruker-Biospin Avance 500 (500 MHz for <sup>1</sup>H NMR) using 5 mm probes and standard pulse sequences. 600 MHz NMR spectra were recorded on a Bruker Avance III spectrometer (Rheinstetten, Germany) equipped with a 5 mm TCI cryoprobe. Standard gradient-enhanced pulse sequences were used for all experiments. Chemical shifts are reported as parts per million (ppm) downfield from tetramethyl silane and are references to the respective solvent signal: CDCl<sub>3</sub> (<sup>1</sup>H:  $\delta$  = 7.26 ppm; <sup>13</sup>C:  $\delta$  = 77.16 ppm); DMSO-*d*<sub>6</sub> (<sup>1</sup>H:  $\delta$  = 2.50 ppm; <sup>13</sup>C:  $\delta$  = 39.52 ppm); Acetone-*d*<sub>6</sub> (<sup>1</sup>H:  $\delta$  = 2.05 ppm; <sup>13</sup>C:  $\delta$  = 206.68 ppm, 29.92 ppm)

### 2.1.3 Data-Processing

The LC-MS data was processed via a rectangular bucketing algorithm (ProfileAnalysis, Bruker, Billerica, MA, USA), integrating the signals of all m/z values from 150 to 600 individually in intervals of 0.5 minutes from minute 1 to 9.5 of chromatographic runtime, forming so called buckets. Most of these buckets consist of measurement noise with no relevant information. Therefore, the next step is to work out those buckets carrying actual signals of eluting peaks, further described as substance or impurity, as each of these buckets should carry the complete integral of a present substance. Accordingly, the complete bucket table was processed via PCA and those substances with high intensity values and inter-sample variation are picked as “key-impurities” carrying the majority of discrimination potential. For the available complex of sixty-one samples of pure **1**, fifteen impurities (**II-II5**) were assessed fulfilling these requirements. The corresponding PCA for assessment of impurities and hierarchical cluster analysis (HCA, using Ward’s method) for sample clustering was computed with the software Unscrambler X (Camo, Oslo, Norway)

## 2.2 Synthesis of MDMB-CHMICA

### 2.2.1 Chemicals and materials

All air- and moisture-sensitive reactions were carried out in oven-dried glassware under an inert atmosphere of nitrogen using standard Schlenk techniques. Removal of solvents was performed using a rotary evaporator (40 °C bath temperature) and a membrane pump. The used solvents were dried and purified by standard procedures. For this purpose, triethylamine (TEA) and dichloromethane (DCM) were distilled from CaH<sub>2</sub>. DMF was purchased in pre-dried quality from Acros Organics and stored over molecular sieves (4 Å). All other chemicals were purchased from commercial suppliers and used without further purification unless mentioned otherwise. For analytical TLC, silica-coated aluminium plates (E. Merck, silica 60 F<sub>254</sub>) and aluminium oxide plates (Marcherey-Nagel, N / UV<sub>245</sub>, ALOX) were used. Details on all instruments used for characterisation of the synthesis intermediates or target compounds can be taken from the supplementary information.

### 2.2.2 Synthesis details

#### *L-tert-Leucine methyl ester hydrochloride*

The title compound was synthesised according to a modified procedure from Imaramovsky et al.<sup>40</sup>

In an oven-dried Schlenk-flask *L-tert-leucine* (500 mg, 3.81 mmol, 1.0 eq) was dissolved in dry methanol (15 mL) and cooled to 0 °C. Subsequently, freshly distilled thionyl chloride (907 mg, 7.62 mmol, 2.0 eq.) was added dropwise at a constant temperature of 5 °C. The clear, yellowish reaction mixture was allowed to reach room temperature by removing the cold bath and stirring vigorously for 40 h. The solvent was removed under reduced pressure and the remaining residue was dissolved again in a mixture of dichloromethane and methanol (10:1). To remove residual *L-tert-leucine*, the solution was filtered over aluminum oxide (Particle size: 50–200 mm, ACROS ORGANICS, Geel, Belgium). The filtrate was acidified with ethereal HCl and evaporated to dryness. *L-tert-Leucine methyl ester hydrochloride* was obtained as colorless crystalline solid. The corresponding analytical characterization can be taken from the supplementary information.

#### *1-(Cyclohexylmethyl)-1H-indole-3-carboxylic acid*

The title compound was synthesised according to an optimized method as part of a classified master's thesis of Steven Hansen. The material was thoroughly purified by flash-chromatography. For a general procedure of the synthesis of 1-(cyclohexylmethyl)-1*H*-indole-3-carboxylic acid refer to Banister et al.<sup>41</sup>. The corresponding analytical characterization data of the product from the stated synthesis can be taken from the supplementary information.

*Methyl (2S)-2-[[1-(cyclohexylmethyl)indole-3-carbonyl]amino]-3,3-dimethylbutanoate (1)*  
(MDMB-CHMICA)

The title compound was synthesised according to a modified procedure from Buchler et al.<sup>34</sup> The coupling conditions for each synthesis are summarized in Table 1.

Coupling via HATU:

A solution of 1-(cyclohexylmethyl)-1*H*-indole-3-carboxylic acid (100 mg, 0.389 mmol, 1.0 eq.) and triethylamine (134.5  $\mu$ L, 0.970 mmol, 2.5 eq.) in DMF (5 mL) was supplemented with HATU (163 mg, 0.43 mmol, 1.1 eq.) and stirred for 15 minutes at room temperature. To the yellow reaction mixture, *L-tert*-leucine methyl ester hydrochloride (106 mg, 0.584 mmol, 1.5 eq.) was added and the mixture was stirred for another 2 h at room temperature.

The reaction mixture was diluted with ethyl acetate (30 mL), washed with HCl (1 mol/L, 2 x 10 mL) and brine (2 x 20 mL), dried (Na<sub>2</sub>SO<sub>4</sub>), and evaporated to dryness, giving a crude yellowish solid (122 mg, 82%).

Coupling via oxalyl chloride and thionyl chloride:

A solution of 1-(cyclohexylmethyl)-1*H*-indole-3-carboxylic acid (50 mg, 0.194 mmol, 1.0 eq.) in DCM (4 mL) was supplemented with oxalyl chloride (20.3 mL, 0.233 mmol, 1.2 eq.) and cooled to 0 °C. Subsequently, DMF was added dropwise (14.63 mL, 0.190 mmol, 0.98 eq.) and stirred for 2 h. *L-tert*-Leucine methyl ester (52.86 mg, 0.291 mmol, 1.5 eq.) and triethylamine (67.23  $\mu$ L, 0.485 mmol, 2.5 eq.) was added and the mixture was stirred for another 2 h at room temperature.

The reaction was stopped by addition of water (5 mL) and conc. NaOH until a pH of 10 was reached. The phases were separated and the organic phase was washed twice with DCM, 0.5 M NaOH and brine (5 mL each). After evaporation to dryness, **1** was obtained as a crude colourless solid (73 mg, 98 %, residues of DMF or TEA might be present).

The complete procedure was repeated with a reaction temperature of 0 °C after the amino acid was added and repeated again, where aliquots of the reaction mixture were taken 1 h, 2 h, 3 h, and 23 h after the amino acid was added.

For the coupling with thionyl chloride, the same reaction conditions were used, except for an addition of thionyl chloride (16.89  $\mu$ L, 0.233 mmol, 1.2 eq) instead of oxalyl chloride.

The corresponding analytical characterization can be taken from the supplementary information.



### 3. Results and Discussion

#### 3.1. Discrimination of seized samples of MDMB-CHMICA based on their impurity signatures

In Münster-Müller et al.<sup>31</sup>, links between forty samples of a large seizure of **1** from Luxembourg customs were worked out via PCA, based on the 57 most abundant impurities found in the corresponding chromatographic impurity signatures. The work was mainly focused on the newly developed workflow of impurity separation and enrichment via F-LC, determination of relative peak areas for a selection of synthesis-related impurities via UHPLC-MS and pattern evaluation via multivariate data analysis, proving the general applicability of the impurity profiling concept for synthetic cannabinoids. In the presented work, the scientific basis for this profiling concept for the synthetic cannabinoid **1** was generated and validated by increasing the analyzed sample set by twenty-one additional samples with no previously known relationship from customs seizures in Finland and internet test-purchases by the University Medical Center Freiburg. It is possible that samples from different sources might be synthesized by another manufacturer, route or under completely different conditions, reflected by the composition and concentration of impurities. No reference material of multiple reaction batches under controlled conditions from the original manufacturer were available which could provide a scientific basis to classify samples of unknown source into individual batches. Thus, the relative distance set for the batch discrimination of the 40 packaging units of the Luxembourg seizure was employed as “calibration distance”. Furthermore, the impurities used for batch discrimination in Münster-Müller et al. were reevaluated<sup>31</sup>. The majority of the 57 impurities detected in the previous study proved to be present in comparatively small concentration or with no inter-sample variation, having minor impact on the statistical model. Therefore, the list of targeted “key-impurities” for **1** was reduced to those fifteen (**I1** to **I15**) with the highest abundance and inter-sample variation, carrying the majority of sample discrimination potential. Although not being a part of the data evaluation, a list of the excluded impurities with expected affiliation to **1** can be taken from the supplemental material. Figure 2 exemplarily shows two overlaid base peak chromatograms (BPC) of the impurity signatures for two unrelated samples of **1** with highlighted impurity peaks **I1** to **I15**, displaying their large fluctuation in abundance and overall relative intensity.

The 15 newly selected “key-impurities” were employed to compare the available seized samples from different sources to reveal potential links. For the samples from the Luxembourg seizure (Lux01 to 40), consisting of forty individual 1 kg packages, a single source/manufacturer is expected and a production batch discrimination was already carried out in a previous publication<sup>31</sup>. This again provides a foundation on which the impurity signatures of samples with no previously known relation can be evaluated when submitted to one chemometric model, in this case eighteen samples seized by Finnish customs (FL01 to 18) and three test purchases in online shops by the University Medical Center Freiburg (FR01 to 03). The table in Figure 3 depicts the impurity signatures for all sixty-one available powder samples of **1**. A greyscale (individual for each impurity) indicates the relative intensities (integrated peak areas of the total ion chromatogram), where white represents a complete absence of signal and black the highest signal value for this impurity. In the last line of the table, the average

intensity ratios between the impurities are compared and normalized to the least abundant to convey their absolute abundances. A hierarchical cluster analysis (HCA) using Ward's method was carried out to group them according to their relative distance in impurity signatures. The resulting dendrogram is attached next to the table for better visual interpretation of the data. No prior normalization was carried out, resulting in the impurities with higher intensity values to be the most influential (e.g. **I15**) for the cluster formation.

Apart from the three outliers (as already reported<sup>31</sup>) Lux14, Lux21 and Lux37, the samples from the Luxembourg seizure form individual clusters of five to ten samples, presumably representing individual synthesis batches. Two of the test purchase samples, FR01 and FR02, also fall into one of these clusters in addition to the fact that both the large seizure and these two test purchased samples were acquired in the same time-frame (end of 2014/ beginning of 2015). Taking into account the relative distance threshold used for batch discrimination of the Lux samples, the similarities in impurity composition for FR01 and FR02 to the Lux samples should not be a coincidence. Possibly, aliquots of the corresponding synthesis batch were sold to the European market before the shipment of the 40 kg order and recovered by chance in form of online test-purchased samples. This hypothesis is validated, as the two test purchase samples fall into the same cluster.

The additional test purchase sample (FR03) from October 2015, seems to be related to FL03, FL09 and FL13-15, which were seized in September-October 2015. Another two clusters consisting of two (FL01-02, seized February 2015, one day apart) and seven (FL04-08, FL11, FL16, seized in the end of 2015) samples can be observed, indicating a common source, possibly even same synthesis batch. The four remaining samples FL10, FL12, FL17 and FL18 cannot be assigned into clusters and stand individually.

### 3.2. Impurities found in seized samples of MDMB-CHMICA

Ten of the fifteen key-impurities could be isolated via F-LC in larger quantities and structural elucidation via HR-MS/MS and NMR was carried out for them. For the remaining five, only HR-MS/MS experiments were performed. All HR-MS and NMR spectra used for structure elucidation are shown in the supplemental material. The corresponding structural formulas of **I1** to **I15** are depicted in Figure 1.

Compound **I1** appears to be a reaction product of *tert*-leucine methyl ester (TLME) and DMF after its oxidative conversion to *N,N*-dimethylcarbamoyl chloride (DMCC) by a chlorinating agent (oxalyl chloride, thionyl chloride or phosphorus oxychloride)<sup>42</sup>. DMF is a common solvent for organic reactions and can be used to catalyze peptide couplings through acyl chloride intermediates<sup>43</sup> and was likely used in the synthesis of the original manufacturer. The fragmentation pattern and exact mass suggest that the structure of compound **I2** consists of at least two *tert*-leucine methyl ester amino acids. With the given MS data, no consistent structure for this impurity could be proposed.

Furthermore, a series of *N*-alkylated amides were identified with carbon chains in different length and branching, in the majority of cases with more than one constitutional isomer in varying intensity ratios. Ions with *m/z* 285 (two isomers), 313 (three isomers), 327 (two

isomers), 341 (three isomers) could be observed, representing the cyclohexylmethyl-substituted indole core with  $\text{NC}_2\text{H}_6$ ,  $\text{NC}_4\text{H}_{10}$ ,  $\text{NC}_5\text{H}_{12}$  and  $\text{NC}_6\text{H}_{14}$  residues bound to the carbonyl linker group, respectively. For  $m/z$  285, two closely eluting isomers with an chromatographic peak area ratio of approximately 1:5 were observed of which the more intense could be isolated and identified as 1-(cyclohexylmethyl)-*N,N*-dimethyl-1*H*-indole-3-carboxamide (**I7**). Since only one other isomer for  $\text{NC}_2\text{H}_6$  is possible, the second, less intense species of  $m/z$  285 is believed to be 1-(cyclohexylmethyl)-*N*-ethyl-1*H*-indole-3-carboxamide. For  $m/z$  313, already seven isomers are possible, three of which were observed, two of them, however, only in trace amounts. The most abundant isomer was isolated and identified as 1-(cyclohexylmethyl)-*N,N*-diethyl-1*H*-indole-3-carboxamide (**I8**). For the remaining two isomers, no structures for the aliphatic portion are proposed, since the amide bond is cleaved in  $\alpha$ -position in the first fragmentation step of MS/MS experiments, giving no additional information about the branching of the carbon chain. None of the isomers of  $m/z$  327 (**I9**) and 341 (**I10**) could be isolated in sufficient amounts and purity for NMR measurements, therefore no further structural information was obtained other than the molecular formulas and fragmentation patterns. Small but significant quantities of triethylamine (TEA) were found in the seized samples from Luxembourg custom<sup>43</sup>, indicating its use as base in the peptide coupling step. It is possible that the TEA used was contaminated with primary and secondary amines of varying branching and chain length resulting in the observed congeners of **1** with aliphatic residues attached to amide bond.

Two nearly co-eluting signals with identical fragmentation patterns of  $m/z$  498 were found in the LC-MS chromatogram of some of the seized samples. With F-LC, it was not possible to isolate both substances individually but only a mixture. Subsequent NMR measurements revealed two highly similar overlapping set of signals for what are most probably two diastereomers of methyl 2-(2-(1-(cyclohexylmethyl)-1*H*-indole-3-carboxamido)-3,3-dimethylbutanamido)-3,3-dimethylbutanoate (**I12**) as reported by Münster-Müller et al.<sup>31</sup> The exact configuration of both isomers is difficult to assess analytically and its formation can have several reasons. In the amino acid reactant, a small concentration of dimers might already have been present, which can undergo an internal rearrangement and epimerization via an 2,5-diketopiperazine (DKP)<sup>44,45</sup>. Since the terminal amino acid in **I12** is present as the methyl ester, the epimerization over a DKP must take place before or during the esterification of *tert*-leucine to *tert*-leucine methyl ester due to loss of the C-terminal ester moiety in the DKP formation. Another possibility is that the amino acid reactant (*tert*-leucine methyl ester) still contains free *tert*-leucine, which is coupled to the 1-(cyclohexylmethyl)-1*H*-indole-3-carboxylic acid residue, providing another carboxylic acid for a second peptide coupling, possibly through a mixed anhydride intermediate. Activated *N*-acyl amino acids are known to epimerize via formation of oxazolonium intermediates<sup>46</sup> followed by coupling of the second amino acid, resulting in an diastereomeric dimer. In any case, the abundance ratio of these two diastereomers was different in all of the seized samples and some of the controlled syntheses. Furthermore, in the syntheses in this study, another constitutional isomer with  $m/z$  498 was found in the trace area of the chromatogram, which had the same molecular formula but a different fragmentation pattern in comparison to the diastereomeric pair. This impurity was not structurally elucidated and is not further considered in this work due to the very small signal intensity. The factors influencing

the ratio of the diastereomers or the formation of the third isomer as well as its structure are still unknown, albeit their presence and ratio seem to be highly discriminating in a batch-to-batch comparison. Unfortunately, the applied bucketing algorithm for automated integration of the LC-MS spectra is not able to distinguish these signals from each other due to the almost identical retention time, summing up the total recorded signal for  $m/z$  498 independent on the number of individual peaks in this close elution range. Therefore, with respect to the profiling, when two samples look similar in their overall impurity signatures generated by this bucketing (numeric values), especially the bucket for  $m/z$  498, an inspection of the LC-MS data (chromatogram and precut ion spectrum of all signals for  $m/z$  498) might provide additional discriminating information before a final conclusion about the relationship of the samples in question is drawn.

Compound **I13** was identified as 5F-MDMB-PICA which itself is a synthetic cannabinoid which was firstly detected on the European market in 2016<sup>47</sup>. The main difference to **1** is the substitution of the N-linked cyclohexylmethyl group with a 5-fluoropentyl chain, which is a common aliphatic residue for various synthetic cannabinoids already on the market (e.g. 5F-PB-22, Cumyl-5F-PINACA, etc.). Speculating about the origin of this impurity, two scenarios are considered. The producers of **1** could have previously synthesized a cannabinoid with a 5F-pentyl chain and residues of 5-fluoropentyl halide remained in the reaction vessels and unintentionally reacted with precursor material of **1**. Alternatively, the manufacturers or a large customer could have contaminated (by accident or on purpose) a large batch of **1** with residues of previously stored MDMB-5F-PICA. In any case, this impurity does not provide information on the synthesis conditions but might be an important marker for its source and is most likely specific for a particular synthesis site or wholesaler. **I13** was present in almost all available powder samples of **1**, leading to the assumption that there is only one large producer and distributor of **1**, responsible for the shipment of the large Luxembourg seizure and distribution of partial quantities of their “contaminated” **1** to vendors around Europe.

One of the most abundant impurities found in the majority of available seized samples of **1** was methyl 2-(2-chloro-1-(cyclohexylmethyl)-1*H*-indole-3-carboxamido)-3,3-dimethylbutanoate (**I15**). In the patented synthesis, no potential chlorine source is used for the indazole-analogue of **1**, apart from simple washing steps with brine or precipitation of intermediates via dil. HCl. Therefore, either the indole used for coupling already contains the chlorine impurity or a reactive chlorinating agent is used for the coupling to the amino acid through the acid chloride. A possible explanation could be an electrophilic reaction attacking the free 2-position of the indole or a radical reaction in which the more stable benzylic radical is formed through attack onto the 2-position which is known for its preference to react with electrophilic radicals. Alternatively, an oxindole impurity in the parent indole-3-carboxylic acid is converted to the 2-chloroindole derivative under dehydrating conditions, which itself would be a redox-neutral process<sup>48</sup>.

Another very insightful contaminant found exclusively in seized **1**, and not in samples prepared under controlled conditions, was **I11**, in which the *tert*-leucine moiety is replaced by 2-aminobutyric acid. It is hard to imagine how a formal double demethylation in the  $\beta$ -position of an amino acid could take place in a non-destructive fashion, so the most probable source of

this impurity is *tert*-leucine itself. A link between *tert*-leucine and 2-aminobutyric acid is the industrial production of these non-proteinogenic amino acids which involves similar multienzyme processes<sup>49,50</sup>. Once the general technology has been established at a given site, the producer can extend its portfolio from one amino acid to the other relatively easily and at least one example of dual production within an otherwise very limited product portfolio is known. Overall, the presence and concentration of this impurity provide information about the purity of the amino acid precursor.

**I14** was characterized as methyl 3,3-dimethyl-2-(1-((tetrahydro-2*H*-pyran-2-yl)methyl)-1*H*-indole-3-carboxamido)butanoate. As for **I12**, the NMR data suggest the presence of two diastereomers with (*R*) and (*S*) tetrahydropyran-2-yl-methyl residues. No valid explanation regarding the formation could be found for this impurity, except for an impure batch of the CHM precursor material or the contamination with a yet unknown experimental cannabinoid. Although other cannabinoid compounds with a structurally related tetrahydropyran-4-yl-methyl residue were already reported (Cumyl-THPINACA<sup>37</sup> or Adamantyl-THPINACA<sup>51</sup>), it is unlikely that their synthesis or distribution stand in any relation to **I14** in form of batch mingling or contaminated synthesis equipment. However, like **I13**, this compound seems to be characteristic for a distinct manufacturer or distributor due to its specific structural element.

Interestingly, several of the structural elements of the impurities (e.g. chlorinated, dimer or *N,N*-dimethyl specimens) were also found in seized samples of other cannabinoids with indole, indazole and carbazole core structures (not published in-house data). As the synthesis of cannabinoids with these core structures can be regarded as modular system, exchanging single structural elements, it seems that the general synthesis procedures such as precursor material or coupling reagents remain constant producing similar types of impurities.

### **3.3. Controlled syntheses on the amino acid coupling step and impact of varied reaction parameters on the impurity profile**

The present profiling routines for classical drugs are based on target impurities, which have been selected according to criteria like discrimination potential or chemical stability<sup>4</sup>. From studies based on controlled syntheses, the appearance and discrimination potential of route-specific by-products as well as the overall reproducibility of the chemical profile can be assessed<sup>20,52</sup>. To better understand differences in seized samples of **1**, the target was to reproduce different scenarios with controlled syntheses that are possible when comparing the impurity signatures of two samples of unknown source. The focus was put on what is expected to be the last reaction step in the synthesis of **1**, the coupling of the amino acid to the alkyl-indole. Larger quantities of 1-(cyclohexylmethyl)-1*H*-indole-3-carboxylic acid were synthesized and cleaned thoroughly. Thus, carry-over from preceding operations should be prevented and all by-products are a result of the ultimate coupling step to the final product. All seized samples of **1** were present in crystalline form and of high purity. It is assumed that the manufacturers purify their final reaction mixture, removing the majority of organic solvents and reactants. Hence, all of the syntheses were worked up with standard extraction protocols (washing with water and brine) until a colorless, crude material was obtained. By-products

were then separated via F-LC and analyzed by UHPLC-MS and HPLC-HR-MS as it was done for the seized material.

By interpreting the impurities found in the seized samples, the following conclusions how to adapt the controlled syntheses starting from the patented version for the indazole analogue from Buchler et al. were drawn: Diisopropylethylamine (Hünig's base) was replaced by TEA, since small quantities of TEA were found in the seized samples<sup>43</sup>. DMF is used either as catalyst or solvent, indicated by the presence of **I1** and the high abundance of the dimethyl isomer of **I7**. And finally, oxalyl chloride was chosen as a coupling agent for two reasons. The highly abundant chlorinated **I15** might be a result of a coupling reaction via an acyl chloride utilizing a chlorinating agent. In addition, considering the economic aspects of the synthesis, coupling via oxalyl chloride on a large scale is much cheaper than using HATU or equivalent<sup>53</sup>.

Different clandestine synthesis scenarios are considered (the expected relations of the corresponding impurity signatures are highlighted in brackets). The samples originate from:

- The same batch. It is expected that these samples show highly similar or even indistinguishable impurity profiles ("strong link"). However, if two aliquots of this batch are stored differently, high temperatures, moisture or exposure to daylight might lead to decomposition. Therefore, the impurity profile of one batch was analyzed directly after synthesis and again after one-month storage either in the freezer or exposure to direct sunlight and room air.
- Different batches, which were prepared under identical conditions ("link"). For this purpose, three batches were prepared and worked up in parallel.
- Different batch syntheses conducted on different days with otherwise identical conditions ("link").
- Different batches prepared with slightly altered reaction parameters, in this study the temperature and time, respectively ("undecided"). One synthesis was carried out with a reaction temperature of 0 °C instead of 25 °C after the amino acid was added. In a second run, aliquots of the reaction mixture were taken and worked up 1 h, 2 h, 3 h and 23 h after the amino acid was added.
- Different batches with different coupling agents ("no-link"). Two more syntheses with thionyl chloride and HATU (as stated in Buchler et al.) as coupling agents were conducted.

All batches were compared on the basis of the previously assessed target impurities in seized samples of **1** (**I1-I15**). Not surprisingly, several impurities found in the seized samples were completely absent in the controlled syntheses, e.g. those with no CHM-substituent attached to the indole (**I3, I4, I5**) or different substituents (**I13, I14**) at this position. All of these products are expected to originate from carry-over of different products from the preceding coupling reaction of CHM to the indole (either incomplete or wrong substituent). Furthermore, any form of chlorinated impurity of **1** was absent in all controlled syntheses. Either the original manufacturers used another coupling agent, such as phosphorus tri- or pentachloride, which were not included in the controlled synthesis experiments, or the reaction mixture was contaminated with catalysts or highly potent reactants leading to oxidation of the indole core,

or an already chlorinated indole is a carry-over from preceding reaction steps. However, in the controlled syntheses several additional reaction by-products were found, never observed in the seized samples (**I16-25**). Since some of these by-products were characteristic for a specific coupling reagent and therefore can be used for batch discrimination, they were implemented in the comparison of the controlled synthesis products and a tentative structural elucidation via MS<sup>n</sup> and HR-MS experiments was carried out. They might be important synthesis pathway markers when investigating the impurity profiles of newly arising synthetic cannabinoids in the future.

Table 1 provides an overview of the conditions for the synthesis variations in this study. All five synthesis variations were carried out in triplicate on the same day. The impact of the different reaction conditions on the target analytes are shown in four bar plots in Figure 4. Each bar in the plots (B)-(D) represents the averaged value of a by-product for the triplicate synthesis with error bars (max and min value).

### 3.3.1 Stability test and comparative analysis of the impurity profile from a single batch of MDMB-CHMICA with oxalyl chloride as coupling reagent

A single finished and worked-up reaction batch of Oxal (**1**) was split into three aliquots for a stability test. The first aliquot was directly submitted to F-LC and the present impurities were assessed by LC-MS to generate a snapshot of the original impurity composition. Another aliquot was stored in a freezer at -20 °C and the last aliquot was stored under sunlight exposure at 25 °C. After a month of exposure, the impurity profiles of both stored samples were reassessed and compared to the profile of the aliquot recorded directly after the synthesis.

No deviation in the impurity composition was observed for the sample stored in the freezer, demonstrating the stability of the main component and the by-products under these conditions. The aliquot exposed to sunlight and air became yellowish after a few days. After one month, LC-MS assessment of the impurity profile showed the presence of two new ions with *m/z* 389 (**I24**; +4 u in comparison to **1**) and 417 (**I25**; +32 u in comparison to **1**). Unfortunately, these substances could not be obtained in sufficient quantities for NMR analysis. The sum formula generated by HR-MS for **I25** was similar to **1** with two additional oxygen atoms most probably attached to or implemented into the indole core. Tryptophan, an amino acid with an indole residue, is known to form *N*-formylkynurenine with elemental oxygen under basic conditions and irradiation with light<sup>54,55</sup>. This might also be the case for the indole core of **1** and would match the recorded fragmentation pattern of **I25**. Additionally, *N*-formylkynurenine is known to form kynurenine via hydrolysis and loss of formic acid<sup>56</sup>, explaining the presence of **I24**, which most probably is the hydrolysis product of **I25**.

After a thorough evaluation of the LC-MS chromatogram of the sample stored in sunlight, no degradation products of any key-impurity could be identified and all signal intensities remained constant. Not surprisingly, **1** as the main component, seems to be most affected by this oxidation. In any case, the characterization of degradation products of the main component might be important for the analytics of indole based synthetic cannabinoids, as these oxidized products might be found as by-products in any seized or purchased samples.

### 3.3.2 Intraday reproducibility with oxalyl chloride as coupling agent

As stated before, all five synthesis variations stated in Table 1 were carried out in triplicate (in parallel, on the same day). The impurity compositions of the three replicates for Oxal (1) are shown in Figure 4 plot (A) as typical example and for illustration purposes. For the remaining four synthesis variations, fluctuations in the impurity composition between the replicates is indicated by error bars for each impurity individually (all bars in plot (B)-(D)).

In general, the replicates of all five synthesis variations exhibited the same set of by-products, albeit with variations in peak areas. In particular the polar substances eluting with short retention times in reverse chromatography like **I2**, **I6** and **I7**, show large fluctuation of abundances. Variations in the washing steps of the reaction mixture with water and brine could result in more or less efficient extraction of these by-products, even though they were carried out as evenly as possible to keep the degree of extraction of water-soluble components equal for all replicates. The aim of the profiling method described in the first part of this study was to discriminate individual synthesis batches of **1** based on the impurity signatures, including **I2**, **I6** and **I7**. If the washing step indeed has an influence on their abundance, these impurities could lose their batch-discriminating potential when multiple aliquots of a single reaction batch are cleaned up differently. However, this scenario is considered unlikely for a large scale production of **1**, which is why it was decided to still include these three compounds as target analytes in the profiling model.

### 3.3.3 Impact of the temperature on the impurity profile and inter-day reproducibility with oxalyl chloride as coupling agent

To compare the inter-day reproducibility and influence of the reaction temperature, Figure 4 (B) shows the by-product signatures for Oxal (1), the 2 h aliquot from Oxal (2) and Oxal (3) with a reduced reaction temperature of 0°C. Apart from the polar components already discussed, comparison of the by-product profiles of Oxal (1) and Oxal (2), at 2h, revealed several other major differences. **I21** was only present in Oxal (1), whereas **I22** was only found in Oxal (2) 2h and **I12** exhibited a five-fold more intense signal. Regarding the differences between the inter-day related variances of Oxal (1) and Oxal (2) 2h, it was difficult to assess variations in the profile as a result of the temperature reduction to 0 °C for Oxal (3). Compared to Oxal (1), an absence of **I2** and **I21** was observed. In any case, both the execution of the synthesis on different days, as well as the reduction of the reaction temperature led to distinguishable by-product signatures.

### 3.3.4 Impact of the reaction time with oxalyl chloride as coupling agent

Oxal (2) was run in triplicate, from which aliquots were taken and worked up after 1 h, 2 h, 3 h, and 23 h after the amino acid was added. The by-product signatures of these aliquots are shown in Figure 4 (C). Some major abundance fluctuations were again observed between the three replicates for the polar components (**I7** in all time aliquots, **I6** after 23 h, **I2** after 3 h and **I19** after 2 and 23 h), making it difficult to draw conclusions about their reaction time dependencies. However, for the abundances of the impurities with aliphatic amine residues of varying length and branching (**I8**, **I9**, **I10** and **I22**), a negative correlation with increased



reaction time was observed. Possibly the sterically unhindered smaller amines react with the activated carboxylic acid faster than the free amino acid. However, after a longer reaction time, more main component was formed. It has to be kept in mind that the dilution factor of the impurity fraction depends on the amount of corresponding isolated main component after F-LC. Because of this increased dilution the signal intensity of the already formed components seem to diminish in relation to the samples taken earlier from the reaction mixture. For **I1** and **I12**, an increased abundance was recorded after 23 h. Obviously, long reaction times favor the formation of amino acid cross reactions, either with the catalyst (DMF) or by formation of dimers. Although a major concentration decrease in the starting material **I6** is expected over long reaction times, in one of the replicates for 23 h this impurity showed a high abundance, possibly due to insufficient washing of the final reaction mixture.

### 3.3.5 Impact of the coupling reagents oxalyl-chloride, thionyl chloride and HATU

Figure 4 (D) shows the by-product signatures produced by the three different amino acid coupling reagents oxalyl chloride (Oxal (1)) thionyl chloride (Thio (4)) and HATU (HATU (5)). The profiles generated by these three coupling reagents are easily distinguishable, only **I1**, **I6** and **I12** showed similar but comparatively low abundances. Two route specific markers **I21** and **I18** were identified for oxalyl chloride. **I2**, with the highest overall abundance, can also be counted among the oxalyl chloride specific markers, although a small signal was also observed in the synthesis with thionyl chloride. **I16**, **I17** and **I20** were specific for a coupling with HATU, via an activated carboxylic acid intermediate and two new by-products with residues of  $\text{NCH}_3$  and  $\text{NC}_3\text{H}_7$  attached to the amide bond, filling the gaps in the homologous series of aliphatically substituted impurities already identified in the seized samples (**I7**, **I8**, **I9** and **I10**). Thionyl chloride did not produce any specific markers, however it gave the highest abundances for three by-products of the homologous series **I8**, **I9** and **I10**. Figure 5 shows an Euler diagram, summarizing which impurities were found in seized samples and samples from the controlled syntheses using different coupling reagents. **I24** and **I25** are excluded from this diagram, as they are the result of forced degradation within the stability studies and are not occurring as the result of the synthesis pathway.

The authors are aware of the fact, that the syntheses were not a perfect reproduction of the original synthesis and this may be reflected in the final impurity profiles. However, considering Oxal (1) or Thio (4) for example, only those seven impurities are absent which are expected to be a result of preceding reaction steps or impure reactants and precursors (considering **I1-I15**). For the controlled synthesis using HATU, four additional impurities, three of which were specific for HATU, and no signals for **I2** and **I10** were observed compared to the seized samples, thus, being the least likely coupling reagent used by the clandestine manufacturer. The coupling with oxalyl chloride also yielded five additional impurities, however, **I21** and **I22**, both oxalyl chloride specific, seem to be formed with a high degree of variation as evidenced by the inter-day reproducibility shown in Figure 4 (B). For thionyl chloride, only two additional impurities were observed in the controlled synthesis and the remaining set of impurities was relatively similar to those of the seized samples. However, for thionyl chloride, only three syntheses were carried out on the same day, providing no information about inter-day reproducibility or change in synthesis conditions. In order to reproduce the complete

profile, all reaction steps would have to be carried out in different sequences with different reagents and conditions. Since it is assumed that syntheses of synthetic cannabinoids consist of at least three steps and no information about the precursor materials is available (in particular which indole core structure is used), extensive synthesis screening would be extremely time-consuming. However, with the given set of information, the authors assume that the coupling step using thionyl chloride seems to be the most likely synthesis procedure of choice for the manufacturing of the seized samples of **1**, although the most abundant impurity **I15** with a chlorine attached to the 2-position of the indole is still absent.

Each of the batches that were synthesized in the survey was discriminable by their by-product signatures. Although the triplicate syntheses carried out in parallel showed the same overall pattern, some signal fluctuations for several impurities could be observed, especially for the polar components. To fully assess the actual impact of the washing steps on the presence of these by-products, further controlled syntheses need to be carried out with a structured series of varying work up-procedures. However, the batch discriminability of the here conducted controlled syntheses validates the batch discrimination assignment carried out for the seized samples as described in the first part of this work and in a previously published work<sup>31</sup>. It was even possible to unambiguously discriminate those syntheses via impurity signatures, which were conducted in parallel.

#### **4. Conclusion**

In this study, fifteen key-impurities in seized samples of MDMB-CHIMCA were assessed and structurally elucidated, of which fourteen were described for the first time. By interpreting the chemical structures of the impurities, a deeper insight into the manufacturing process of synthetic cannabinoids was obtained. 61 samples of pure MDMB-CHMICA from customs seizures and internet test purchases were grouped by multivariate data analysis of their impurity patterns. This provides a powerful tool for impurity profiling of synthetic cannabinoids to acquire basic information about the distribution and market structures by analyzing and grouping powder samples from different sources. To further strengthen the discrimination power of the impurity profiling concept, the impurity patterns could be combined in a unified chemometric model with isotope ratio mass spectrometry (IRMS) data as orthogonal analytical information providing additional information about the origin of precursor material. It appears that the impurity profiles of samples seized or bought in similar time-frames tend to match. Possibly, the manufacturers of **1** produce individual batches depending on the demand of their recipients and ship them to Europe consecutively.

As second part of this study the reaction by-products in a set of controlled syntheses of a synthetic cannabinoid were investigated to better understand variations in impurity signatures and to assess the significance of variations in the impurity patterns of seized samples in order to establish links between them. Eight new by-products were identified in the products of the controlled syntheses and two additional decomposition compounds formed in the subsequent stability tests. All of the eight new by-products were not present in any of the 61 investigated seized samples and showed high abundances or discriminating potential for a specific synthesis pathway. The coupling via thionyl chloride was the most likely synthesis route used by the

clandestine manufacturer, as only two additional impurities were formed in the controlled synthesis. However, still a few of the key-impurities found in the seized material could not be reproduced by the different controlled synthesis approaches, like the chlorinated derivative of **1**, suggesting that the clandestinely applied synthesis procedure has not yet been identified in minute detail. The aspects of single-batch discriminability, inter- and intra-day reproducibility, the influence of the reaction temperature and time and, lastly, the influence of the coupling agent were investigated. Regarding the inter-day reproducibility, statistically relevant differences in impurity patterns were found, which, however, is a positive aspect for the applicability of batch-to-batch comparison as performed in the first part of this study. The degree of variations in the impurity profile correlated with the magnitude of variation in synthesis reaction parameters which, thus, provides a reliable evidence base for the assignment of sample relations based on impurity signatures of the synthetic cannabinoid MDMB-CHMICA targeted in this study.

### **Author information**

*Corresponding Author*

\* Sascha Münster-Müller, sascha.muenster-mueller@uni-rostock.de

### **Notes**

We confirm that this manuscript has not been published elsewhere or is under review by another journal. All authors have approved the manuscript and agree with submission to Drug Testing and Analysis. Furthermore, no competing financial interest or safety considerations are declared by the Authors.

### **Acknowledgments**

All presented data, if not cited otherwise, were generated within the project “SPICE-profiling”, funded within the EU’s ISEC 2013 programme (Directorate-General JUST/2013/ISEC/DRUGS/AG/ISEC/4000006421). Again, our thanks are due to Serge Schneider from the Laboratoire National de Santé in Luxembourg, who kindly provided us with aliquots from the large seizure of MDMB-CHMICA by Luxembourg customs, Ildary Szilvay for providing aliquots seized by the Finnish Customs, and Volker Auwärter and Verena Angerer from the University Medical Centre Freiburg for supplying samples from internet test purchases. Furthermore, we want to thank Dieter Kirsch, Steven Luhn and Vincent Guillou from the Federal Criminal Police, Forensic Science Institute in Germany for their help with HR-MS and NMR measurements.

### **Supporting Information**

- Analytical data (MS and NMR) used for structural characterization of impurities
- Analytical characterization of synthesis intermediates and target compounds
- List of additional impurities found in seized samples of MDMB-CHMICA

## References

1. Ehleringer JR, Casale JF, Lott MJ, Ford VL. Tracing the geographical origin of cocaine. *Nature*. 2000;408:311.
2. Janzen KE, Fernando AR, Walter L. A database for comparison analysis of illicit cocaine samples. *Forensic Sci. Int.* 1994;69(1):23-29.
3. Janzen KE, Walter L, Fernando AR. Comparison analysis of illicit cocaine samples. *J. Forensic Sci.* 1992;37(2):436-445.
4. Ballany J, Caddy B, Cole M, et al. Development of a harmonised pan-European method for the profiling of amphetamines. *Sci. Justice*. 2001;41(3):193-196.
5. Hauser F, Rößler T, Hulshof J, Weigel D, Zimmermann R, Pütz M. Identification of specific markers for amphetamine synthesised from the pre-precursor APAAN following the Leuckart route and retrospective search for APAAN markers in profiling databases from Germany and the Netherlands. *Drug Test Anal.* 2018;10(4):671-680.
6. Pikkarainen AL. Systematic approach to the profiling analysis of illicit amphetamine. *Forensic Sci. Int.* 1996;82(2):141-152.
7. Sinnema A, Verweij AM. Impurities in illicit amphetamine: review. *Bull. Narc.* 1981;33(3):37-54.
8. UNODC. *Drug Characterization/Impurity profiling*. Vienna: UNODC; 2001. Available from: <https://www.unodc.org/pdf/publications/st-nar-32-rev1.pdf>. Accessed 26. March 2019.
9. Chiarotti M, Marsili R, Moreda-Pineiro A. Gas chromatographic-mass spectrometric analysis of residual solvent trapped into illicit cocaine exhibits using head-space solid-phase microextraction. *J. Chromatogr. B Analyt. Technol. Biomed. Life Sci.* 2002;772(2):249-256.
10. Zacca JJ, Grobério TS, Maldaner AO, Vieira ML, Braga JWB. Correlation of cocaine hydrochloride samples seized in Brazil based on determination of residual solvents: an innovative chemometric method for determination of linkage thresholds. *Anal. Chem.* 2013;85(4):2457-2464.
11. Zhang JX, Zhang DM, Han XG. Identification of impurities and statistical classification of methamphetamine hydrochloride drugs seized in China. *Forensic Sci. Int.* 2008;182(1-3):13-19.
12. Palhol F, Boyer S, Naulet N, Chabrillat M. Impurity profiling of seized MDMA tablets by capillary gas chromatography. *Anal. Bioanal. Chem.* 2002;374(2):274-281.
13. Stromberg L, Lundberg L, Neumann H, Bobon B, Huizer H, van der Stelt NW. Heroin impurity profiling. A harmonization study for retrospective comparisons. *Forensic Sci. Int.* 2000;114(2):67-88.
14. Perkal M, Ng YL, Pearson JR. Impurity profiling of methylamphetamine in Australia and the development of a national drugs database. *Forensic Sci. Int.* 1994;69(1):77-87.
15. Power JD, Kavanagh P, McLaughlin G, et al. Forensic analysis of P2P derived amphetamine synthesis impurities: identification and characterization of indene by-products. *Drug Test Anal.* 2017;9(3):446-452.
16. Kunalan V, Nic Daéid N, Kerr WJ, Buchanan HAS, McPherson AR. Characterization of route specific impurities found in methamphetamine synthesized by the Leuckart and reductive amination methods. *Anal. Chem.* 2009;81(17):7342-7348.
17. Doughty D, Painter B, Pigou P, Johnston MR. The synthesis and investigation of impurities found in clandestine laboratories: Baeyer-Villiger route part II; synthesis of Phenyl-2-propanone (P2P) analogues from substituted benzaldehydes. *Forensic Chemistry*. 2018;9:1-11.

18. Toske SG, Cooper SD, Morello DR, Hays PA, Casale JF, Casale E. Neutral heroin impurities from tetrahydrobenzylisoquinoline alkaloids. *J. Forensic Sci.* 2006;51(2):308-320.
19. Stojanovska N, Fu S, Tahtouh M, Kelly T, Beavis A, Kirkbride KP. A review of impurity profiling and synthetic route of manufacture of methylamphetamine, 3,4-methylenedioxyamphetamine, amphetamine, dimethylamphetamine and p-methoxyamphetamine. *Forensic Sci. Int.* 2013;224(1):8-26.
20. Aalberg L, Andersson K, Bertler C, et al. Development of a harmonized method for the profiling of amphetamines. I. Synthesis of standards and compilation of analytical data. *Forensic Sci. Int.* 2005;149(2-3):219-229.
21. Toske SG, McConnell JB, Brown JL, et al. Isolation and characterization of a newly identified impurity in methamphetamine synthesized via reductive amination of 1-phenyl-2-propanone (P2P) made from phenylacetic acid/lead (II) acetate. *Drug Test Anal.* 2015;9(3):453-461.
22. Aalberg L, Andersson K, Bertler C, et al. Development of a harmonised method for the profiling of amphetamines: II. Stability of impurities in organic solvents. *Forensic Sci. Int.* 2005;149(2):231-241.
23. Dujourdy L, Dufey V, Besacier F, et al. Drug intelligence based on organic impurities in illicit MA samples. *Forensic Sci. Int.* 2008;177(2-3):153-161.
24. UNODC. *Impurity profiling of heroin and cocaine*. Vienna: UNODC; 2005. Available from: [https://www.unodc.org/pdf/publications/report\\_st-nar-35.pdf](https://www.unodc.org/pdf/publications/report_st-nar-35.pdf). Accessed 26. March 2019.
25. Collins M, Doddridge A, Salouros H. Cathinones: Isotopic profiling as an aid to linking seizures. *Drug Test Anal.* 2016;8(9):903-909.
26. Münster-Müller S, Scheid N, Holdermann T, Schneiders S, Pütz M. Profiling of new psychoactive substances by using stable isotope ratio mass spectrometry: Study of the synthetic cannabinoid 5F-PB-22. *Drug Test Anal.* 2018;in press.
27. Schäffer M, Gröger T, Pütz M, Zimmermann R. Assessment of the presence of damiana in herbal blends of forensic interest based on comprehensive two-dimensional gas chromatography. *Forensic Toxicol.* 2013;31(2):251-262.
28. UNODC. *Current NPS Threats*. Vienna: UNODC; 2019. Available from: [https://www.unodc.org/pdf/opioids-crisis/Current NPS Threats - Volume I.pdf](https://www.unodc.org/pdf/opioids-crisis/Current_NPS_Threats_-_Volume_I.pdf). Accessed 26. March 2019.
29. Auwärter V, Dresen S, Weinmann W, Müller M, Pütz M, Ferreirós N. 'Spice' and other herbal blends: harmless incense or cannabinoid designer drugs? *J. Mass Spectrom.* 2009;44(5):832-837.
30. Langer N, Lindigkeit R, Schiebel H-M, Papke U, Ernst L, Beuerle T. Identification and quantification of synthetic cannabinoids in "spice-like" herbal mixtures: Update of the German situation for the spring of 2016. *Forensic Sci. Int.* 2016;269:31-41.
31. Münster-Müller S, Zimmermann R, Pütz M. A novel impurity-profiling workflow with the combination of flash-chromatography, UHPLC-MS, and multivariate data analysis for highly pure drugs: a study on the synthetic cannabinoid MDMB-CHMICA. *Anal. Chem.* 2018;90(17):10559-10567.
32. EMCDDA. *Synthetic cannabinoids in Europe (Perspectives on drugs)*. Lisbon: EMCDDA; 2017. Available from: [http://www.emcdda.europa.eu/system/files/publications/2753/POD\\_Synthetic%20cannabinoids\\_0.pdf](http://www.emcdda.europa.eu/system/files/publications/2753/POD_Synthetic%20cannabinoids_0.pdf). Accessed 26. March 2019.
33. EMCDDA. *Report on the risk assessment of MDMB-CHMICA in the framework of the Council Decision on new psychoactive substances*. Lisbon: EMCDDA; 2017. Available from:

[http://www.emcdda.europa.eu/system/files/publications/4093/TDAK16002ENN\\_PDF WEB.pdf](http://www.emcdda.europa.eu/system/files/publications/4093/TDAK16002ENN_PDF_WEB.pdf). Accessed 26. March 2019.

34. Buchler P, Indazole derivatives. WO2009106980, 2009.
35. Huffman JW, Dai D, Martin BR, Compton DR. Design, synthesis and pharmacology of cannabimimetic indoles. *Bioorg. Med. Chem. Lett.* 1994;4(4):563-566.
36. Makriyannis A, Hongfeng D, Cannabimimetic indole derivatives. US6900236 B1, 2005.
37. Bowden M, Williamson J, Cannabinoid Compounds. WO2014167530, 2014.
38. Weber C, Pusch S, Schollmeyer D, Münster-Müller S, Pütz M, Opatz T. Characterization of the synthetic cannabinoid MDMB-CHMCZCA. *Beilstein J. Org. Chem.* 2016;12:2808-2815.
39. Uchiyama N, Matsuda S, Kawamura M, Kikura-Hanajiri R, Goda Y. Two new-type cannabimimetic quinolinyl carboxylates, QUPIC and QUCHIC, two new cannabimimetic carboxamide derivatives, ADB-FUBINACA and ADBICA, and five synthetic cannabinoids detected with a thiophene derivative  $\alpha$ -PVT and an opioid receptor agonist AH-7921 identified in illegal products. *Forensic Toxicol.* 2013;31(2):223-240.
40. Imramovsky A, Jorda R, Pauk K, et al. Substituted 2-hydroxy-N-(arylalkyl)benzamides induce apoptosis in cancer cell lines. *Eur. J. Med. Chem.* 2013;68:253-259.
41. Banister SD, Longworth M, Kevin R, et al. Pharmacology of valinate and tert-leucinate synthetic cannabinoids 5F-AMBICA, 5F-AMB, 5F-ADB, AMB-FUBINACA, MDMB-FUBINACA, MDMB-CHMICA, and their analogues. *ACS Chem. Neurosci.* 2016;7(9):1241-1254.
42. Stare M, Laniewski K, Westermark A, Sjögren M, Tian W. Investigation on the formation and hydrolysis of N,N-dimethylcarbonyl chloride (DMCC) in vilsmeier reactions using GC/MS as the analytical detection method. *Org. Process Res. Dev.* 2009;13(5):857-862.
43. Andernach L, Pusch S, Weber C, et al. Absolute configuration of the synthetic cannabinoid MDMB-CHMICA with its chemical characteristics in illegal products. *Forensic Toxicol.* 2016;34(2):344-352.
44. Gaines SM, Bada JL. Aspartame decomposition and epimerization in the diketopiperazine and dipeptide products as a function of pH and temperature. *J. Org. Chem.* 1988;53(12):2757-2764.
45. Nitecki DE, Halpern B, Westley JW. Simple route to sterically pure diketopiperazines. *J. Org. Chem.* 1968;33(2):864-866.
46. Davies JS, Mohammed AK. Assessment of racemisation in N-alkylated amino-acid derivatives during peptide coupling in a model dipeptide system. *J. Chem. Soc., Perkin Trans. 1.* 1981(0):2982-2990.
47. Risseuw MDP, Blanckaert P, Coopman V, Van Quekelberghe S, Van Calenbergh S, Cordonnier J. Identification of a new tert-leucinate class synthetic cannabinoid in powder and "spice-like" herbal incenses: Methyl 2-[[1-(5-fluoropentyl)indole-3-carbonyl]amino]-3,3-dimethyl-butanoate (5F-MDMB-PICA). *Forensic Sci. Int.* 2017;273:45-52.
48. Powers JC. Chloroindoles. *J. Org. Chem.* 1966;31(8):2627-2631.
49. Tao R, Jiang Y, Zhu F, Yang S. A one-pot system for production of l-2-aminobutyric acid from l-threonine by l-threonine deaminase and a NADH-regeneration system based on l-leucine dehydrogenase and formate dehydrogenase. *Biotechnol. Lett.* 2014;36(4):835-841.
50. Menzel A, Werner H, Altenbuchner J, Gröger H. From enzymes to "designer bugs" in reductive amination: a new process for the synthesis of L-tert-leucine using a whole cell-catalyst. *Eng. Life Sci.* 2004;4(6):573-576.

51. Asada A, Doi T, Tagami T, Takeda A, Sawabe Y. Isomeric discrimination of synthetic cannabinoids by GC-EI-MS: 1-adamantyl and 2-adamantyl isomers of N-adamantyl carboxamides. *Drug Test Anal.* 2017;9(3):378-388.
52. Schwemer T, Rössler T, Ahrens B, et al. Characterization of a heroin manufacturing process based on acidic extracts by combining complementary information from two-dimensional gas chromatography and high resolution mass spectrometry. *Forensic Chemistry.* 2017;4:9-18.
53. Dunetz JR, Magano J, Weisenburger GA. Large-scale applications of amide coupling reagents for the synthesis of pharmaceuticals. *Org. Process Res. Dev.* 2016;20(2):140-177.
54. Nakagawa M, Watanabe H, Kodato S, et al. A valid model for the mechanism of oxidation of tryptophan to formylkynurenine—25 years later. *Proc. Natl. Acad. Sci. U. S. A.* 1977;74(11):4730-4733.
55. Saito I, Matsuura T, Nakagawa M, Hino T. Peroxidic intermediates in photosensitized oxygenation of tryptophan derivatives. *Acc. Chem. Res.* 1977;10(9):346-352.
56. Dreaden TM, Chen J, Rexroth S, Barry BA. N-formylkynurenine as a marker of high light stress in photosynthesis. *J. Biol. Chem.* 2011;286(25):22632-22641.

Accepted Article

**Table 1** List of the controlled synthesis variations with corresponding parameters for the last reaction step (coupling of the amino acid) for MDMB-CHMICA. Each synthesis was run in triplicate in parallel.

Name	Coupling agent	Solvent	Base	Catalyst	Temp.	Time	Replicates
Oxal (1)	Oxalyl chloride	DCM	TEA	DMF	25 °C	2 h	3
Oxal (2)	Oxalyl chloride	DCM	TEA	DMF	25 °C	1 h, 2 h, 3 h, 23 h	3
Oxal (3)	Oxalyl chloride	DCM	TEA	DMF	0 °C	2 h	3
Thio (4)	Thionyl chloride	DCM	TEA	DMF	25 °C	2 h	3
HATU (5)	HATU	DMF	TEA	-	25 °C	2 h	3

Accepted Article



# Accepted Article

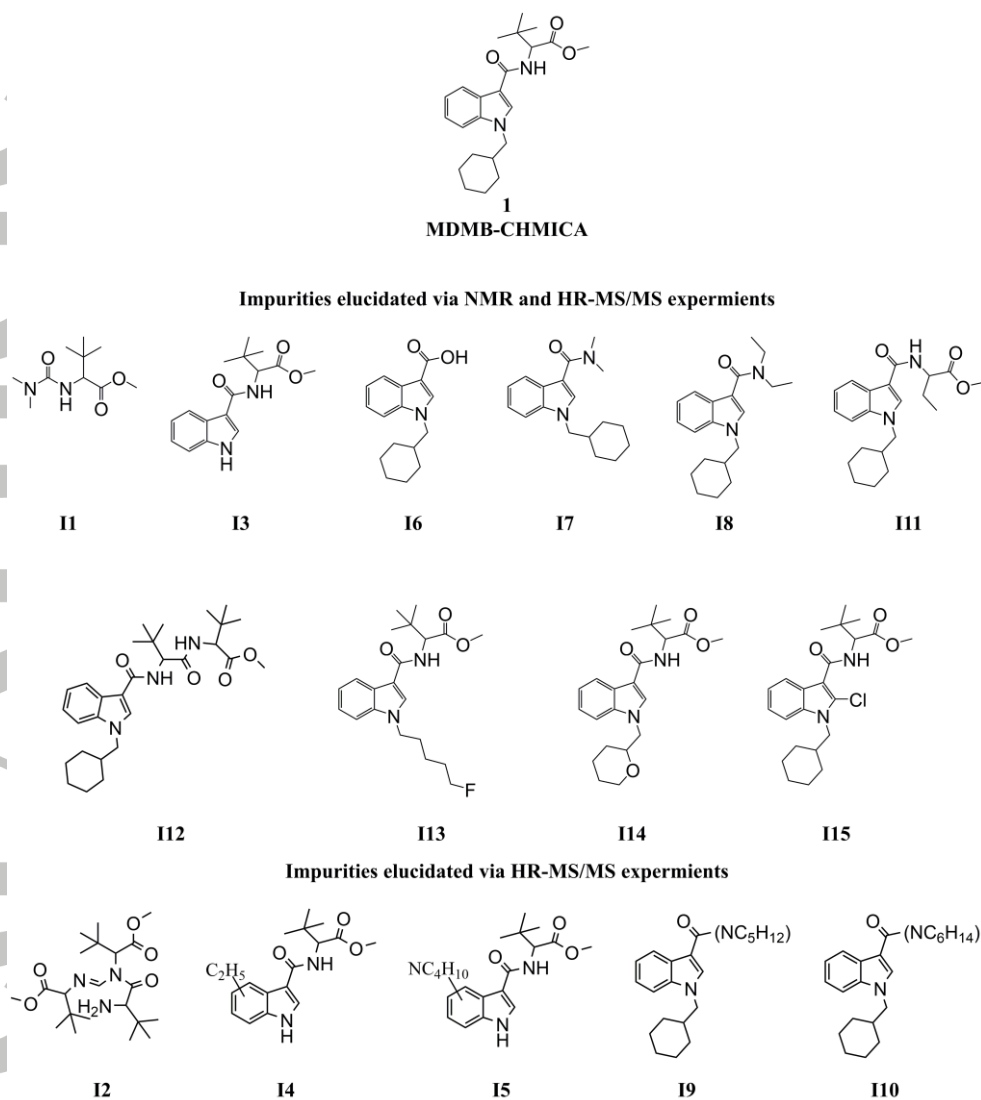


Figure 1. Structural formulas for MDMB-CHMICA and fifteen assessed key-impurities with high discriminating potential to distinguish between individual synthesis batches in seized samples. Five impurities were only elucidated via HR-MS/MS experiments, the remaining ten were characterized by both NMR and HR-MS experiments.

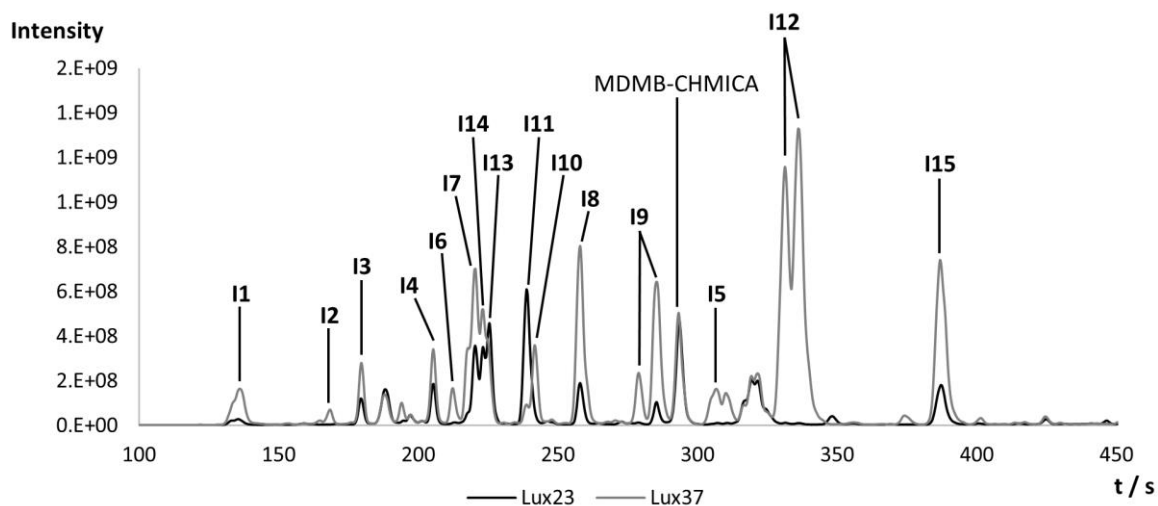


Figure 2. Overlaid UHPLC-MS base peak chromatograms (BPCs) of impurity signature for two MDMB-CHMICA samples. The impurity peaks carrying the most discrimination potential to distinguish between samples are numbered from I1-I15.

Accepted Article

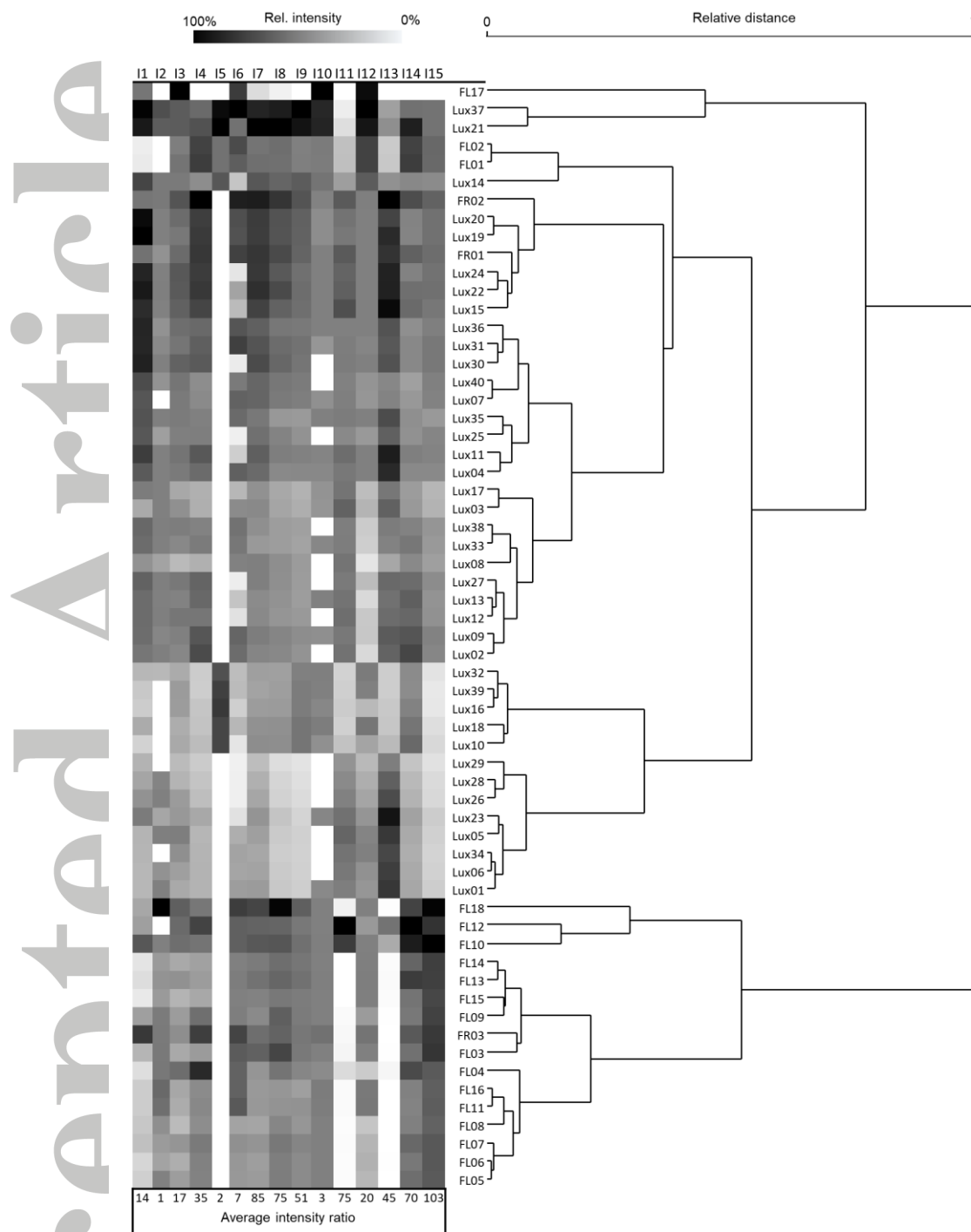


Figure 3. Table (left) with impurity signatures for 61 powder samples of MDMA, with a greyscale individual for each impurity that indicates the relative integrated peak areas measured in each sample, where white represents a complete absence of signal and black the highest signal value for this impurity. The relative intensity ratio between the impurities is indicated in the last row to convey their absolute abundances. The dendrogram (HCA, Ward's method, right) shows the calculated relative distance between the samples on the basis of their impurity signatures.

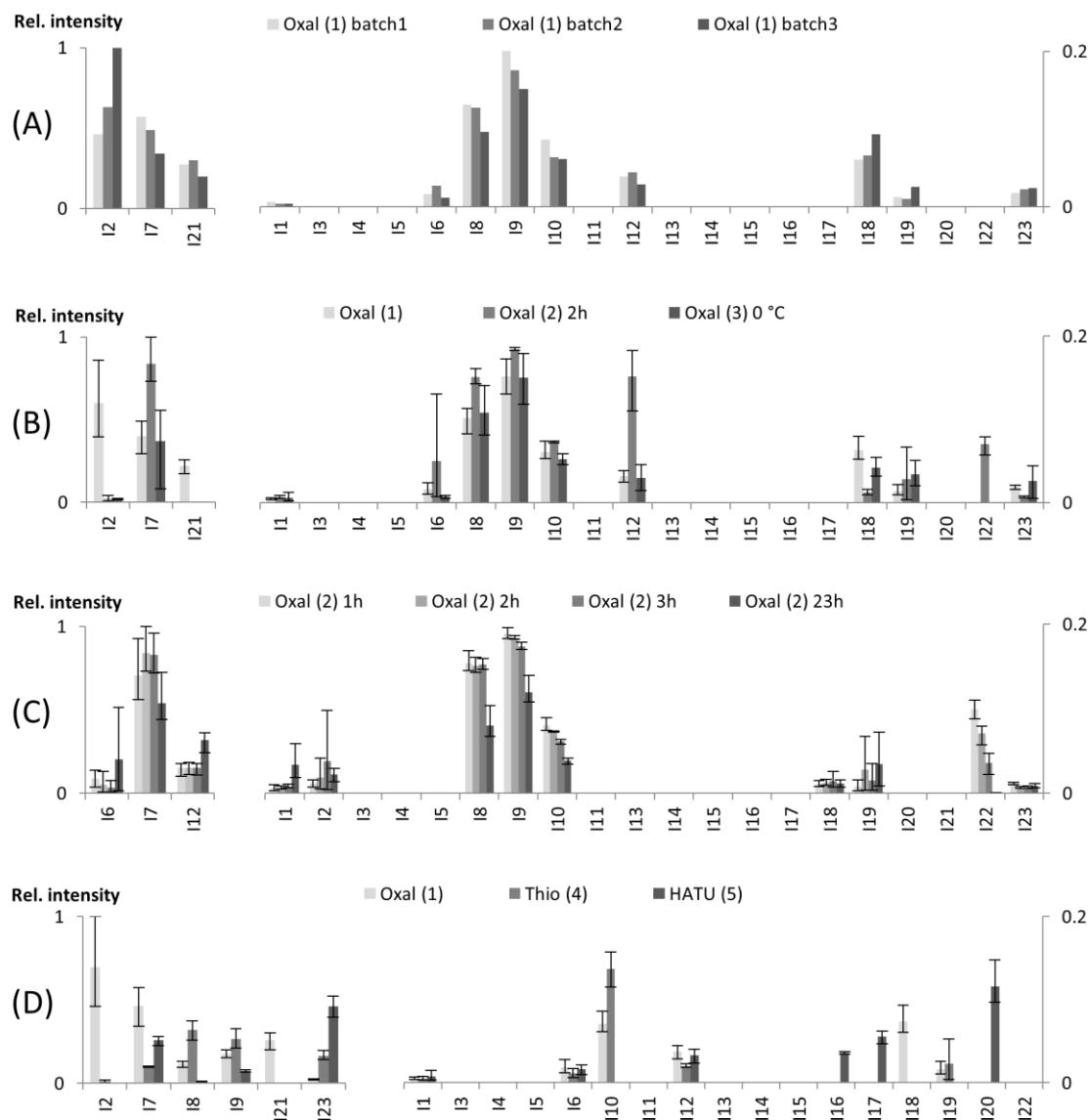


Figure 4. Bar plots of the by-product signatures of controlled synthesis of MDMB-CHMICA. (A) Three batches of Oxal (1) run in parallel with identical conditions. (B) Oxal (1), Oxal (2) 2h with identical conditions conducted on different days. Additionally, Oxal (3) conducted on a different day with reduced reaction temperature to 0 °C. (C) Four aliquots of Oxal (2) taken from the reaction mixture after the reaction was started (1h , 2h, 3h, 23h). (D) Couplings via the reagents oxalyl chloride (Oxal (1)), thionyl chloride (Thio (4)) and HATU (HATU (5)).

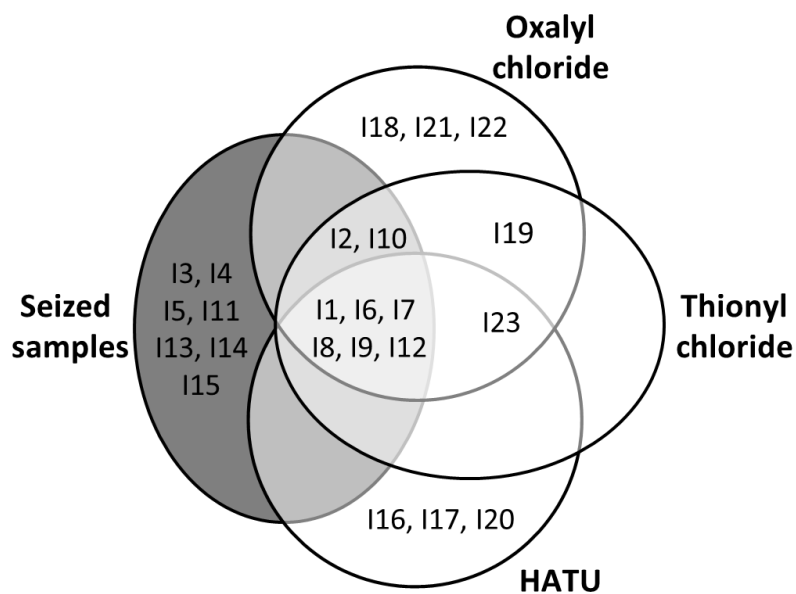
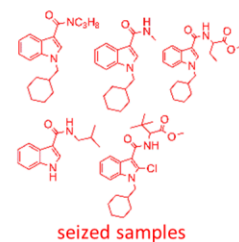
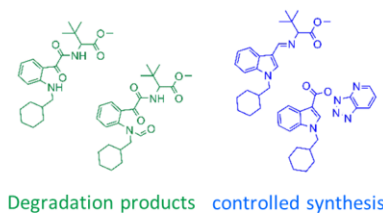
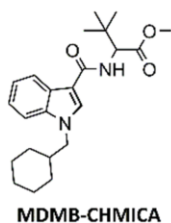


Figure 5. Euler diagram of the key impurities I1 to I15, assessed in seized samples of MDMB-CHMICA, and I16 to I23, found in controlled syntheses of the amino acid coupling using the three different coupling reagents HATU, thionyl chloride and oxalyl chloride

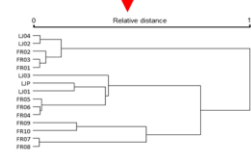
# Chemical profiling of the synthetic cannabinoid MDMB-CHMICA: identification, assessment and stability study of synthesis-related impurities in seized and synthesized samples

Sascha Münster-Müller\*, Steven Hansen, Till Opatz, Ralf Zimmermann and Michael Pütz

We investigated and characterized the most discriminating synthesis-related impurities found in samples from seizures and controlled synthesis of the synthetic cannabinoid MDMB-CHMICA. On their basis, sixty-one seized samples of MDMB-CHMICA were evaluated and classified via multivariate data analysis. Stability tests and multiple controlled syntheses of MDMB-CHMICA were carried out to better understand variations in impurity signatures and to assess the significance of variations in the impurity patterns of seized samples.



Semi-quantitative analysis



Multivariate data evaluation

Accepted Article